15 Jan 2014

Environmental Stress Cracking of Glassy Polymers

Parthasakha Neogi
Missouri University of Science and Technology, neogi@mst.edu

Gholamreza Zahedi

Recommended Citation

P. Neogi and G. Zahedi, "Environmental Stress Cracking of Glassy Polymers," *Industrial and Engineering Chemistry Research*, vol. 53, no. 2, pp. 672 - 677, American Chemical Society, Jan 2014.
The definitive version is available at https://doi.org/10.1021/ie403201a

I&EC research
Industrial & Engineering Chemistry Research

Article

pubs.acs.org/IECR

Environmental Stress Cracking of Glassy Polymers

Parthasakha Neogi* and Gholamreza Zahedi

Chemical and Biochemical Engineering, Missouri University of Science and Technology, Rolla, Missouri 65409-1230, United States

ABSTRACT: When a glassy polymer is exposed to an organic solvent, it can crack spontaneously or fail more readily under extension. This is environmental stress cracking. When the solvent diffuses into the polymer, stresses develop because of swelling of the polymer. In addition, fluctuations give rise to stresses, because of the variation in surface tension from changes in the surface concentration of the solute, which is the Marangoni effect. A linear stability analysis is performed to show that such a system is unstable to infinitesimal disturbances. Large tensile stresses arise locally, leading to failures, which will be observed in the interfacial region of the solid. In particular, the unstable disturbances of smaller wavelengths grow faster. This is consistent with the observation that the microscopic cracks that emanate from the surface are more profuse in cracks that are more closely spaced as seen in experiments.

INTRODUCTION

When a solid polymer is exposed to a vapor or a liquid, it can crack spontaneously or fail at low extension. In most cases, the polymer is glassy and the fluid is a solvent for polymer. One example is shown in Figure 1. Commercial poly(methyl methacrylate) (PMMA) was dipped into liquid acetone for a short period and then dried and kept on a filter paper overnight. The result was severe cracking, and the phenomenon is the most common case of environmental stress cracking.[1,2] A look at the failures shows that it has a characteristic length scale associated with the distance between visible cracks that are not fully random. There are actually two sets of cracks, one for each surface. If the cracks emanate from the surface, then the density of the cracks on the surface becomes very important in the failure of the material,[3] where such cracks do not have to be deep. Thus, a high density of surface cracks could also explain the easier material failure upon extension.[4] Environmental stress cracking constitutes a way in which polymeric materials get compromised and limit their use. The recent review by Robeson[5] shows that environmental stress cracking has remained an important problem; it discusses the preventive methods used and new types of environmental stress cracking encountered particularly on new polymers. However, not much in quantification has been added beyond Bernier and Kambour's[4] correlation with solubility parameters. Use of stresses in understanding sorption in polymer membranes is not new. The basic scheme is available in Larché and Cahn[6] and has been developed or adapted variously to study anomalous sorption in glassy polymers.[7−13]

From the point of view of visualizing the phenomenon, Kambour[14] suggested that, when a solute enters the polymer, the stress concentration at the interface between swollen and unswollen polymer increases, causing the cracks. Most suggested mechanisms on environmental stress cracking rely on the match between the solubility parameters of the polymer and the fluid.[4,15−18] That is, Bernier and Kambour[4] plotted the ease of failure for a fixed polymer treated with various liquids, in the form of extension at which failure takes place ε versus the solubility parameter δ. They observed ε to have a minimum in δ. Some researchers have integrated the mechanics of crack growth to the solubility parameters.[19,20] Yet others have related the crack growth to diffusion of the fluid molecules into the polymer.[21] No quantitative model exists that couples stresses to the mass-transfer process.

The mechanism that couples the effects of surface tension to stresses that are generated spontaneously is given below. It is known that the surface tension is a function of local concentration and can give rise to interfacial instability, called the Marangoni instability. Existing problems deal with liquid-fluid systems.[22] The mechanism has been extended here to cover fluid−solid systems. When the system is unstable, large stresses can be generated locally and lead to failure. Thus, the effects of surface tension have been added to the existing coupled problem between mass transfer and stress.[6] The dynamics of solids is well-known and much of the details, where they follow the work of Kolsky,[23] have been omitted.

Base Case. The constitutive equation is the Kelvin or Vogt model. The key difference introduced by Larché and Cahn[6] is that the strain tensor is given by

$$\mathbf{E} = \mathbf{E}^{m} + \mathbf{E}^{c} \tag{1}$$

where $\mathbf{E}^{m}$ is the mechanical part of the deformation and $\mathbf{E}^{c}$ is the deformation due to the chemical part and is generally taken to be isotropic:

$$\mathbf{E}^{c} = \frac{1}{3} tr(\mathbf{E}^{c})\mathbf{I} \tag{2}$$

where the trace $tr(\boldsymbol{E}^{c}) = \Delta V^{c}/V_0$, where ΔV^{c} is the change in volume due to swelling and V_0 is a reference volume. The trace is usually set to $\omega(c - c_0)$, where ω is a constant. Furthermore, setting the reference state as that of the dry polymer leads to ωc only where c is the concentration of the solute. It is the form $\mathbf{E}^{m} = \mathbf{E} - \mathbf{E}^{c}$ that is used in the constitutive equation to obtain stress, which is then used in the momentum balance equation. The strain, in terms of deformation $\boldsymbol{u}$, is given as

Received: September 26, 2013
Revised: December 4, 2013
Accepted: December 12, 2013
Published: December 20, 2013

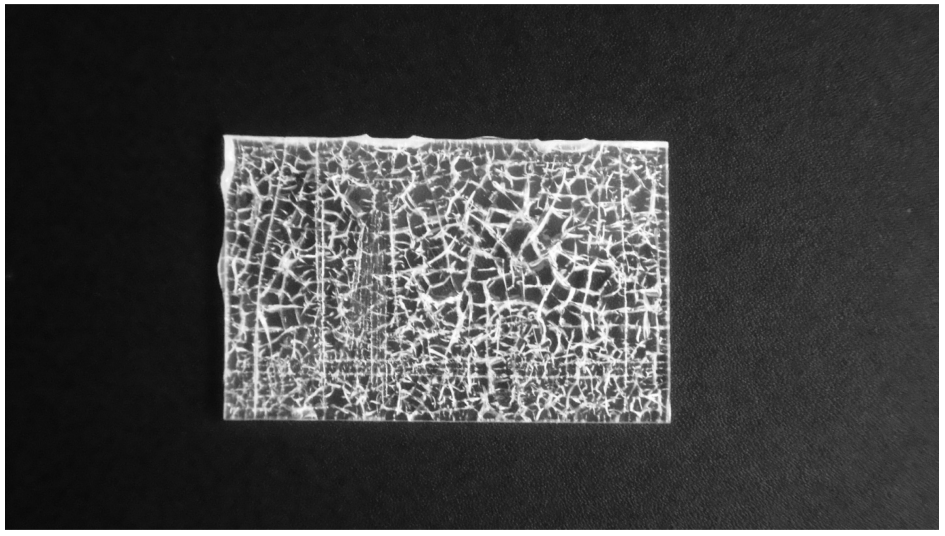

Figure 1. Photograph of commercial poly(methyl methacrylate) (PMMA) contacted with acetone, leading to failure. The scratches on the surface were made to determine if the cracks on the surface had any depth (they apparently do not). Besides the visible cracks, the surfaces contain many more microscopic cracks. The width of the sample is 3.1 mm.

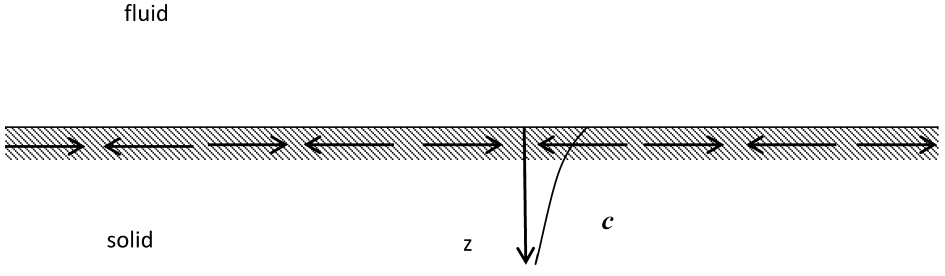

Figure 2. The coordinate system and the nature of the key forces at the surface.

$$\mathbf{E} = \frac{1}{2}[\nabla\mathbf{u} + (\nabla\mathbf{u})^{\mathrm{T}}] \tag{3}$$

and eventually the momentum balance equation becomes

$$\rho_0\frac{\partial^2\mathbf{u}}{\partial t^2} = \left(\lambda + \lambda_v\frac{\partial}{\partial t}\right)\nabla(\nabla\cdot\mathbf{u}) + \left(\mu + \mu_v\frac{\partial}{\partial t}\right)[\nabla^2\mathbf{u} + \nabla(\nabla\cdot\mathbf{u})] - \left[\lambda + \lambda_v\frac{\partial}{\partial t} + \frac{2}{3}\left(\mu + \mu_v\frac{\partial}{\partial t}\right)\right]\omega\nabla c \tag{4}$$

where the Lamé constants λ and μ were defined as follows:

$$\lambda = \frac{\nu E}{(1+\nu)(1-2\nu)}$$

and

$$\mu = \frac{E}{2(1+2\nu)}$$

where E is the Young's modulus and ν is the Poisson's ratio. Furthermore, μ_v is the bulk shear viscosity ($\mu_v = \eta$) and $\lambda_v = \kappa - (2/3)\eta$, given that κ is the bulk dilatational viscosity.

A conservation of species equation in the solid is also needed, in the form

$$\frac{\partial c}{\partial t} + \mathbf{v}\cdot\nabla c = \nabla\cdot(D_s\nabla c) \tag{5}$$

where the velocity $\boldsymbol{v} = \partial\boldsymbol{u}/\partial t$ and the diffusivity in the solid (D_s) is strongly concentration-dependent.

We need boundary conditions, and that is where the effects of surface tension comes in.[22] Kolsky[23] provides the solution to eq 4 (less the concentration effects) in the form of waves that do not show instability in the form of growing stresses. We feel that the introduction of the surface tension into the problem will do so. It is this solution that is considered in the next section.

Figure 2 shows the interface given by $z = 0$ and the coordinate system with solid (s) on one side and fluid (f) on the other. The fluid can be a solution containing the solute or the solute in pure form. Interest here lies in the very short time following the initial contact. The concentration of the solute in the bulk fluid is c_b or c_b^0 if pure. The solution to the mass-transfer problem is straightforward and leads to a flux N:

$$c_b = N\left[\sqrt{\frac{\pi t}{D_f}} + \frac{1}{Kk_i} + \frac{1}{K}\sqrt{\frac{\pi t}{D_s(0)}}\right] \tag{6}$$

where the boundary condition at the solid/liquid interface is

$$N = k_i(Kc_i - c_{si}) \tag{7}$$

where $1/k_i$ is the interfacial mass-transfer resistance. If $1/k_i = 0$, then local equilibrium takes place at the interface as K is the equilibrium partition coefficient. Equation 6 also applies when the fluid phase is pure, in which case, the left-hand side becomes c_b^0 and D_f is set to infinity.

Stability Analysis. The effect of fluctuations is now considered. These fluctuations occur in all quantities and are related to each other through conservation equations and

dx.doi.org/10.1021/ie403201a | Ind. Eng. Chem. Res. 2014, 53, 672−677

boundary conditions. Fluctuations are assumed to change rapidly and take place over small length scales such that the base case described above remains unchanged. All fluctuations that are very small and allow linearization are confined to the interfacial region and decay in the interiors. The linear differential equations that result are solved in a straightforward manner. Consider first the fluctuations in concentration. The diffusivity in the fluid is assumed to be large, thus diffusion will restore any fluctuation in concentration to the base value c_b and is omitted from consideration. The fluctuating quantities will be denoted by primes. Hence, $c_s = \bar{c}_s + c_s'$ and eq 7 becomes

$$N' = k_i(Kc_b - c_{si})' = -k_i c_{si}' - k_i \frac{\partial \bar{c}_s}{\partial z}\cdot z' \tag{8}$$

where z' is the new position of the interface. Equation 5 is similarly perturbed and simplified with a diffusivity

$$D_s = D_0 e^{\alpha c_s} \tag{9}$$

as is the boundary condition that $\boldsymbol{u}c_s\cdot\boldsymbol{n} - \boldsymbol{n}\cdot D_s\nabla c_s = N$, where $\boldsymbol{n}$ is the unit normal to the interface.

We carry out the perturbations along with the assumed solution in the form

$$c_s' = a(z)e^{i\chi y}e^{\beta t} \tag{10}$$

$$u_z' = b(z)e^{i\chi y}e^{\beta t} \tag{11}$$

where $i = \sqrt{-1}$ and $z' = u_z'$ at $z = 0$, and we obtain, from eq 5,

$$a'' + 2\alpha\frac{\partial \bar{c}_s}{\partial z}a' - a\left[\chi^2 + \frac{\beta}{D_0} - \alpha\frac{\partial^2 \bar{c}_s}{\partial z^2}\right] = \left(\frac{\beta}{D_0}\right)\frac{\partial \bar{c}_s}{\partial z}b \tag{12}$$

where primes denote differentiation with z. It is assumed that the fluctuations change spatially much faster than the base quantities; hence, the derivatives of $\bar{c}_s$ in z are treated as constants. The solution is substituted into the boundary condition described by eq 8, which becomes

$$k_i a + k_i\frac{\partial \bar{c}_s}{\partial z}b + \beta b c_{si} = D_0\left(\alpha a\frac{\partial \bar{c}_s}{\partial z} + \frac{da}{dz}\right) + D_0\left(\alpha\frac{\partial \bar{c}_s}{\partial z} + \frac{\partial^2 \bar{c}_s}{\partial z^2}\right)\cdot b \qquad \text{at } z = 0 \tag{13}$$

An additional simplification of setting $e^{\alpha c} = 1$ has been made at the very end of the calculations to arrive at the above two equations.

As a preview, we note that the final goal is to determine β. If the rate of growth β is positive, then the system is unstable to very small disturbances, as those will grow with time. If it is negative, then the system is stable. χ, which is the wavenumber of disturbance, is given as $\chi = 2\pi/(\text{wavelength of the disturbance})$.

The momentum equation (eq 4) is solved by taking divergence and curl to get two differential equations for dilation and shear,[22] which are taken, respectively, to be

$$\Phi = de^{i\chi x}e^{\beta t} \tag{14}$$

$$\Psi = fe^{i\chi x}e^{\beta t} \tag{15}$$

where d and f are unknown functions of z. These equations are solved and substituted in the boundary conditions below.

The two key boundary conditions are of normal stress balance

$$\sigma_{zz}' = \left(\lambda + \lambda_v\frac{\partial}{\partial t}\right)\nabla^2\Phi + 2\left(\mu + \mu_v\frac{\partial}{\partial t}\right)\frac{\partial u_z'}{\partial z} - \left[\lambda + \lambda_v\frac{\partial}{\partial t} + \frac{2}{3}\left(\mu + \mu_v\frac{\partial}{\partial t}\right)\right]\omega c' = \gamma\frac{\partial^2 z'}{\partial x^2} \tag{16}$$

and the shear stress and stress balance is

$$\sigma_{xz}' = \left(\mu + \mu_v\frac{\partial}{\partial t}\right)\left(\frac{\partial u_x'}{\partial z} + \frac{\partial u_z'}{\partial x}\right) = \gamma_c\frac{\partial c'}{\partial x} \tag{17}$$

where γ is the surface tension, which multiplies the approximate form of curvature suitable for small displacements and $\gamma_c = \partial\gamma/\partial c$ (which is assumed to be a constant), is usually negative. Both eqs 16 and 17 are evaluated at $z = 0$ and the surface tension and mass-transfer terms have been introduced for the first time in the problem of surface waves discussed by Kolsky.[23]

Solution. The resulting problem is very large and some simplifications are sought to enable us to interpret the results more closely. One of them is $\partial\bar{c}_s/\partial z$ and $\partial^2\bar{c}_s/\partial z^2$ are neglected and λ_v and μ_v are set to zero. The results obtained hold only for short times and do not contain any damping effects since the viscosities have been removed. The solutions to the differential equations lead to

$$a = A_2e^{-qz} \tag{18}$$

$$d = A_3e^{-nz} + A_4e^{-qz} \tag{19}$$

$$f = A_1e^{-mz} \tag{20}$$

and

$$b = d' - i\chi f \tag{21}$$

where A_1, A_2, and A_3 remain unknown and $A_4 = \Lambda A_2$, where

$$\Lambda \approx \frac{(2/3)\omega}{(\beta/D_0) + (8/3)(\beta^2/s^2)}$$

with $s^2 = E/\rho$. In addition,

$$q = \sqrt{\chi^2 + \frac{\beta}{D_0}}$$

$$n^2 = \chi^2 + \frac{\rho\beta^2}{\lambda + \lambda_v\beta + 2(\mu + \mu_v\beta)}$$

$$m^2 = \chi^2 + \frac{\rho\beta^2}{(\mu + \mu_v\beta)}$$

The result, when using the boundary conditions, can be written as

$$\underline{\underline{a}}\,\underline{A} = \underline{0} \tag{22}$$

where $\underline{\underline{a}}$ is a 3×3 matrix and $\underline{A}$ is a column vector of A_1, A_2, and A_3. For the solution to be nontrivial, the determinant of $\underline{\underline{a}}$ must vanish. This leads to

$$\det(\underline{\underline{a}}) = 0 \tag{23}$$

which gives us the dispersion equation of $\beta(\chi)$.

dx.doi.org/10.1021/ie403201a | Ind. Eng. Chem. Res. 2014, 53, 672−677

The issue is now to calculate the value of β. The usual practice is to nondimensionalize the dispersion equation and solve for dimensionless β as a function of dimensionless χ. However, there are many parameters (dimensionless groups) in the system that make it very difficult to interpret numerical results. Another procedure is to set $\beta = 0$ and calculate the value of χ_m for this marginal stability case. However, the dispersion equation contains imaginary terms, hence χ_m will be complex, making it again difficult to analyze the result. It is possible to show that there are two very disparate length scales (or time scales). One of these arises from the slow diffusivity D_0, and the other results from the fast speed of sound s; hence, q is approximated as $q \approx (\beta/D_0)^{1/2}$ and Λ has also been approximated. These are all the approximations that can be made. It becomes important to scan wavelengths from the large wavelength to the small wavelength. Numerical results and what they predict are discussed next.

RESULTS AND DISCUSSION

We assume a diffusivity of $D_0 \approx 10^{-6}$ cm^2/s,[24] $E \approx 3 \times 10^9$ N/m^2, and $\nu = 1/3$ for glassy polymers,[25,26] with a density of $\rho \approx 0.8$ g/cm^3. These values lead to an estimate of $s \approx 1.87 \times 10^5$ cm/s and $L_D = (8/3)^{1/2} D_0/s \approx 5.3 \times 10^{-12}$ cm. Taking $\gamma \approx 30$ mN/m[27] gives $L_\gamma = \gamma/E \approx 1.07 \times 10^{-9}$ cm. If a low concentration on the surface is ~100 mM, then c_{si} with a molecular weight of 70 is 7×10^{-3} g/cm^3, and with $\omega \approx 0.62$ in mass units,[28] $\omega c_{si} \approx 4.34 \times 10^{-3}$. A value of $\gamma \approx 30$ mN/m has been used to calculate L_γ above, but γ for the solid−liquid system, a value of $\gamma \approx 5$ mN/m is used to calculate dimensionless $p = \gamma_c c_{si}/\gamma = \Delta\gamma/\gamma$, using a value of $\Delta\gamma \approx -1$ mN/m. Thus, $p \approx -0.2$. Finally, we assume a value of $k_i \approx 10$ m/s, which is a very large quantity.[29]

Since χ is the wavenumber of the disturbance, it should range from 1 cm^{-1} to 10^8 cm^{-1}, with corresponding wavelengths of 6.3 cm to 6.3×10^{-8} cm, such that the sample size is not exceeded nor are molecular dimensions crossed. For a given χ, we have looked for those values of dimensionless β of $\kappa = (8/3)^{1/2}\, \beta/(\chi s)$, where $Re(\kappa) > 0$ using Matlab. Only one such value (and sometimes none) could be found, as shown in Figure 3. The wavenumber χ where $\beta \propto \kappa\chi$ is the largest, is ~87 000 cm^{-1}, leading to a wavelength of 110 nm, which is less than the wavelength of visible light, although disturbances of larger wavelengths, which are of importance from a practical point of view, are also shown to be unstable but grow very slowly. The trend that the disturbances of small wavelengths grow faster, is clear.

When the strength of the surface tension gradient $p \approx -0.033$ is decreased by a factor of 6, the rate of growth decreases by 5 orders of magnitude (compare Figures 3 and 4). It should be mentioned that Figure 4 involves a lower value of $k_i \approx 1$ cm/s which should increase the rate of growth of instability as large k_i tends to suppress fluctuations in surface concentrations. Nevertheless, this feature is overshadowed by a decrease in the magnitude of p. We find that p and $\partial\gamma/\partial c = \gamma_c$ are required to be negative for the instability to take place and vanishes when they reach zero.

Now, however, the swelling introduced by the solute generates compressive stresses,[8] as can be ascertained by the negative stress. Such a stress can cause buckling of the interface. Although we have not investigated this mode of instability, we have ascertained that, when $\omega = 0$, there is no swelling and Marangoni instability still takes place. In fact, it has been shown that, with swelling, stresses can be actually relieved,[9] because

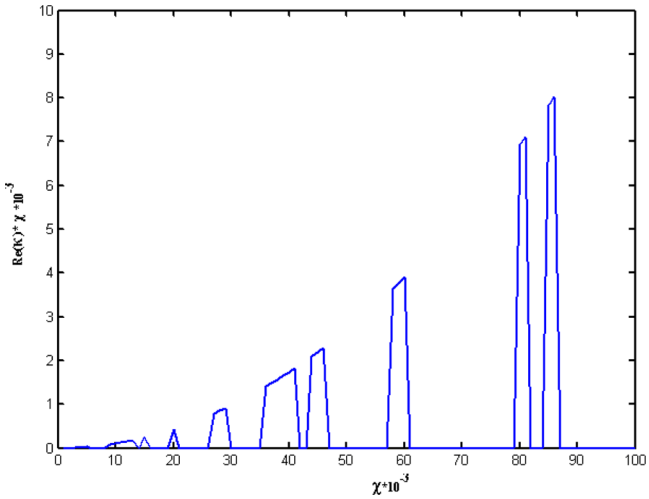

Figure 3. The rate of growth β is proportional to $\kappa\chi$, the real part of which has been plotted against the wavenumber χ. There is only one such root for κ, where the real part is positive. For many values of χ, there is no such root. The region on the right-hand side shown here has no such roots. Here, $p = -0.2$ and $k_i/D_0 = 10^9$ cm^{-1}.

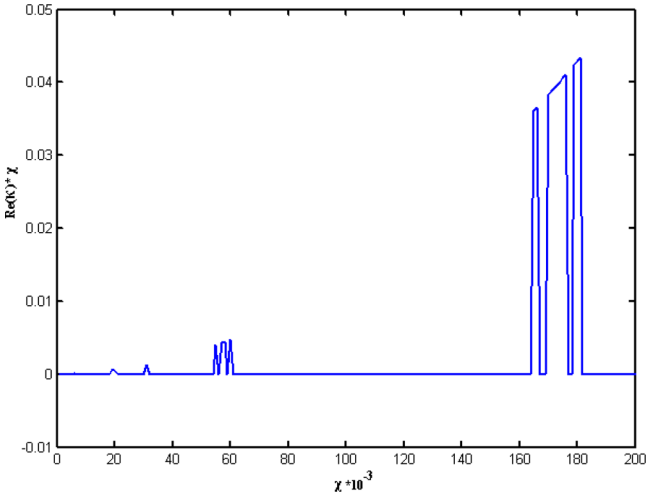

Figure 4. Similar to Figure 3, the real part of $\kappa\chi$ has been plotted against χ. Here, $p = -0.033$ and $k_i/D_0 = 10^6$ cm^{-1}.

the lowered Young's modulus, which is due to the presence of the solute, allows much larger deformations without raising the stress.

The regions to the right in Figures 3 and 4 have no solutions. This is the stabilizing influence of surface tension which, however, is not very effective, because γ is so low and E is so large. Disturbances of large χ (small wavelengths) greatly increase the interfacial area and the surface free energy, and the surface tension acts to eliminate these disturbances. If we look at γ/E, its gives us a representative length scale over which these two forces balance each other: ~10^{-9}−10^{-8} cm. This is the wavelength below which the system should be stable. We find the system to be well-stabilized above this value (~10^{-5} or 2×10^{-5} cm, below which no unstable solutions could be found). On the other side, the disturbances of χ in the 1−100 cm^{-1} range, where effects are visible to the naked eye, are also unstable, but their rates of growth are very small for both cases.

Experimental observation that the cases where the gap between adjacent cracks is the smallest (<1 mm) is most

dx.doi.org/10.1021/ie403201a | Ind. Eng. Chem. Res. 2014, 53, 672−677

profuse, is reported in the Appendix. The cause of instability is that the tangential stresses in eq 17 cannot be balanced. This is shown schematically in Figure 2. Looking at forces shown there, it is obvious that there are regions of tensile stresses, and materials fail more readily in tension, leading to cracks. The distance between adjacent cracks will be the wavelength used here. Now, as seen in Figures 3 and 4, the fastest growing wavelengths will be the smallest ones (110 nm in Figure 3). If we look at a relatively large unstable wavelengths, then two adjacent cracks will be separated by this large distance. However, the disturbances of smaller wavelengths will give rise to many cracks in between making the first pair undetectable. But no intervening cracks are expected in a pair of cracks separated by the fastest growth wavelength, that is, the smallest wavelength. Consequently, if we measure the distances between adjacent cracks, then these distances will be biased toward small ones, as seen in the Appendix.

The coupling between mass and momentum persists in eq 13, even when k_i is infinite, provided no additional assumptions are made. With this coupling and the Marangoni effect, instability is expected, although it has not been pursued here. It is also possible to suggest that the case considered here also includes the case where the solute is available in the form of a solution and not a pure phase. Using local equilibrium for simplicity, eq 7 is replaced with

$$N = k_L\left(c_b - \frac{c_{si}}{K}\right) \tag{24}$$

where k_L is the mass-transfer coefficient on the fluid side and K is a partition coefficient. Furthermore,

$$N' = -\left(\frac{k_L}{K}\right)c_s'\Big|_{z=0} - \left(\frac{k_L}{K}\right)\frac{\partial \bar{c}_s}{\partial z}\Big|_{z=0}\cdot z' \tag{25}$$

By comparison with N' preceding eq 8, we can substitute k_i with k_L/K in all the results that follow.

Bernier and Kambour's[4] plot in critical extension ε versus solubility parameter δ shows a minimum as mentioned earlier, however, the minimum is asymmetric. The environmental stress cracking disappears when δ falls below the minimum by 1.5 $cal^{1/2}$ $cm^{2/3}$ but survives for ~10 above this minimum. The surface tension of a mixture for a very simple system[21] can be written as $\gamma \approx x_1\gamma_1 + x_p\gamma_p$, where x is the mole fraction, subscript 1 represents the penetrant, and p represents the polymer. Consequently, $\partial\gamma/\partial c \propto (\gamma_1 - \gamma_p)$. It points to the dissymmetry mentioned earlier as only negative values of $\gamma_1 - \gamma_p$ gives rise to the environmental stress cracking. There are many theories that relate the surface tension to the solubility parameter, common one being $\gamma \propto \delta^2$ which can be used to show that $\partial\gamma/\partial c \propto (\delta_1 - \delta_p)$ assuming that the two δ values are not too far apart and using Taylor's expansion. Now, $\delta_1 - \delta_p$ to the first approximation is proportional to the square root of the Flory–Huggins polymer-penetrant interaction parameter. Gent[17] showed that Bernier and Kambour's ε correlated quite well with Flory–Huggins parameter, which has also been verified by Mai.[18] At $\delta_1 = \delta_p$, we have a good solvent and in addition leads to $\gamma_1 = \gamma_p$, and zero $\partial\gamma/\partial c$. Hansen[15] has observed that good solvents are not good cracking agents, and in our model no cracking will occur in this case. We also point out that the relationships established here will see significant modification or even overridden if the fact that glasses are nonequilibrium system is considered, and if the facts that one or both components can be polar and the sizes of the two molecules quite disparate. Data, however, support the idea that the basic model is close.

CONCLUSIONS

Marangoni instability arises when a glassy polymer is contacted with a fluid that dissolves in the solid (such as a solvent for the polymer). The phenomenon in solids, instead of flow as in liquids, leads to cracking which is known to be far quicker than the dissolution process. The distance between adjacent cracks is favored to be small.

APPENDIX

A thin plate of commercial poly(methyl methacrylate) (PMMA) was machined at one end, as shown in Figure A1.

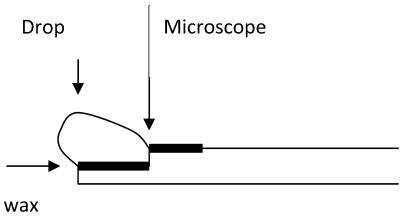

Figure A1. Schematic depiction of the experimental setup. The liquid drop is acetone and can contact only the vertical face of the ledge of the PMMA plate ~2 mm thick.

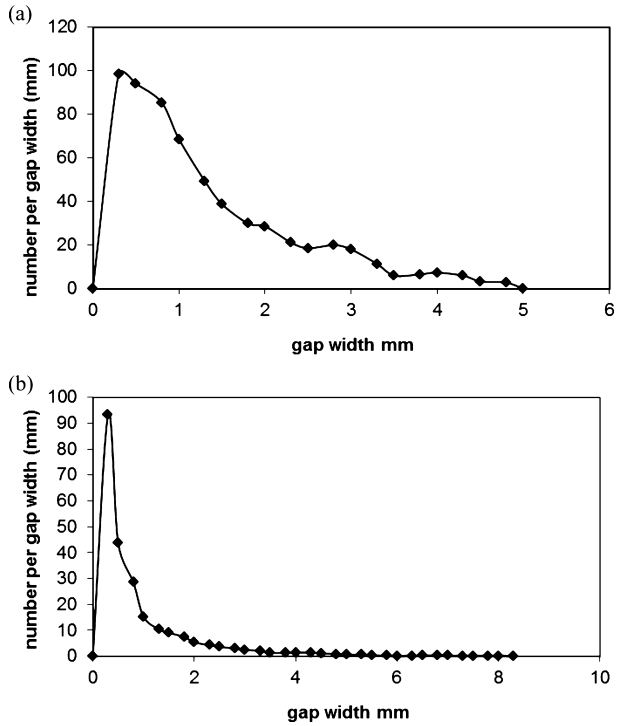

Figure A2. Number densities of the distribution are shown for two samples. The number of cases with adjacent cracks at separation (in mm) shown on the x-axis: (a) acetone and (b) butyl acetate.

After machining, it was checked under a microscope to see if cracks appeared. There were no small cracks but a few samples were chipped and had to be rejected. Only the vertical edge was left untouched; however, wax was applied on the other faces at this end. Acetone (or butyl acetate) was deposited on the ledge, such that the vertical surface was directly exposed. All other surfaces were waxed. The surface was viewed from the top

dx.doi.org/10.1021/ie403201a | Ind. Eng. Chem. Res. 2014, 53, 672–677

under a microscope after a day. The edge was profuse with cracks that were microscopic. The distances between two adjacent cracks were measured, where all such distances below 1 mm were lumped together. The distribution for two samples are shown in Figure A2. The preponderance of very small crack separation is obvious. Qualitatively, at a level visible to the naked eye, both acetone and butyl acetate showed large cracks that were separated at distances greater than those shown in Figure A2. The fact that, with so many cracks, the material will fail more readily under tension, is obvious.

AUTHOR INFORMATION

Corresponding Author

*Tel.: (573) 341-4460. Fax: (573) 341-4377. E-mail: neogi@mst.edu.

Notes

The authors declare no competing financial interest.

ACKNOWLEDGMENTS

P.N. acknowledges the assistance of Mathew Z. Griscom and Tracy E. Downs in preparing the Appendix.

REFERENCES

(1) Andrews, E. H. Cracking and crazing in polymeric glass. In *The Physics of Glassy Polymer*; Haward, R. N., Ed.; Applied Science: London, 1973; p 394.

(2) Ubberreiter, K. The solution process. In *Diffusion in Polymers*; Crank, J., Park, G. S., Eds.; Academic Press: New York, 1968; p 220.

(3) (a) Hu, K. X.; Chandra, A. Interactions amongst the cracks and rigid lines near a free surface. *Int. J. Solids Structures* **1993**, *30*, 1919. (b) Lubarda, V. A.; Krajcinovic, D. Damage tensors and the crack density distribution. *Int. J. Solids Structures* **1993**, *30*, 2859.

(4) Bernier, G. A.; Kambour, R. P. Craze formation yield stress and the so-called ductile–brittle transition in glassy polymers. *Macromolecules* **1968**, *1*, 190.

(5) Robeson, L. M. Environmental stress cracking: A review. *Polym. Eng. Sci.* **2013**, *53*, 453.

(6) Larché, F. C.; Cahn, J. W. The effect of self-stress on diffusion in solids. *Acta Metall.* **1982**, *30*, 1835.

(7) Kim, M.; Neogi, P. Concentration-induced stress effects in diffusion of vapors through polymer membranes. *J. Appl. Polym. Sci.* **1984**, *29*, 731.

(8) Neogi, P. Diffusion in solids under strain, with emphasis on polymer membranes. *AIChE J.* **1986**, *32*, 1146.

(9) Neogi, P. Nonlinear elastodiffusion at small deformations in polymer membranes. *Chem. Eng. Commun.* **1988**, *68*, 185.

(10) Camera-Roda, G.; Sarti, G. S. Non-Fickian mass transfer through polymers: A viscoelastic theory. *Transport Theory Stat. Phys.* **1986**, *15*, 1023.

(11) Doghieri, F.; Sarti, G. S. Mass transport and mechanical properties of solid polymers. *Makromol. Chem. Macromol. Symp.* **1993**, *68*, 257.

(12) Camera-Roda, G.; Sarti, G. C. Mass transport with relaxation in polymers. *AIChE J.* **1990**, *36*, 851.

(13) Lustig, S. P.; Caruthers, J. M.; Peppas, N. A. Continuum thermodynamics and transport theory for polymer–fluid mixtures. *Chem. Eng. Sci.* **1992**, *47*, 3037.

(14) Kambour, R. P. Mechanistic aspects of crazing and cracking of polymers in aggressive environments. In *Mechanisms of Environmental Stress Cracking of Materials*; Swann, P. R., Ford, F. P., Westwood, A. R. C., Eds.; The Metal Society: London, 1977; p 213.

(15) Hansen, C. M. On predicting environmental stress cracking in polymers. *Polym. Degrad. Stab.* **2002**, *77*, 43.

(16) Hansen, C. M.; Just, L. Prediction of environmental stress cracking in plastics with Hansen solubility parameters. *Ind. Eng. Chem. Res.* **2001**, *40*, 21.

(17) Gent, A. N. Hypothetical mechanism of crazing in glassy polymers. *J. Mater. Sci.* **1970**, *5*, 925.

(18) Mai, Y.-W. Environmental stress cracking of glassy polymers and solubility parameters. *J. Mater. Sci.* **1986**, *21*, 904.

(19) Andrews, E. H.; Bevan, L. Mechanics and mechanism of environmental crazing in a polymeric glass. *Polymer* **1972**, *13*, 337.

(20) Williams, J. G.; Marshall, G. P. Environmental crack and craze growth phenomena in polymers. *Proc. R. Soc. London A* **1975**, *342*, 55.

(21) Hay, J. N.; Kemmish, D. J. Environmental stress crack resistance of absorption of low-molecular-weight penetrants by poly(aryl ether ether ketone). *Polymer* **1988**, *29*, 613.

(22) Miller, C. A.; Neogi, P. *Interfacial Phenomena. Equilibrium and Dynamic Effects*. CRC Press: Boca Raton, FL, 2008; pp 36, 307.

(23) Kolsky, H. *Stress Waves in Solids*; Dover Publications: New York, 1963 (originally published by Clarendon Press, Oxford, U.K., 1953).

(24) Vrentas, J. S.; Duda, J. L. Molecular diffusion in polymer solutions. *AIChE J.* **1979**, *25*, 1.

(25) Haward, R. N. The nature of polymeric glasses, their packing densities and mechanical behavior. In *The Physics of Glassy Polymers*; Haward, R. N., Ed.; Applied Science: London, 1973; p 1.

(26) Ferry, J. D. *Viscoelastic Properties of Polymers*, 3rd Ed.; John Wiley: New York, 1980; p 437.

(27) Zisman, W. A. Relation of the equilibrium contact angle to liquid and solid constituents. In *Contact Angle, Wettability, and Adhesion*, Gould, R. F., Ed.; American Chemical Society: Washington, DC, 1964; p 1.

(28) Jefferies, R. The thermodynamic properties of mixtures of secondary cellulose acetate and its solvent. *Trans. Faraday Soc. 1* **1957**, *53*, 592.

(29) Sherwood, T. K.; Pigford, R. L.; Wilke, C. R. *Mass Transfer*; McGraw–Hill: New York, 1975; pp 148, 301.